

# Well-defined skeletal macroporous polymer monoliths fabricated with a novel type of amphiphilic diblock copolymer as a phase separator

Peiyong Xin<sup>a,b</sup>, Li Qi<sup>a,\*</sup>, Rongyue Zhang<sup>a,b</sup>, Chunhe Yao<sup>a,b</sup>, Xiaoyi Wei<sup>a,b</sup>, Gengliang Yang<sup>c</sup>, Yi Chen<sup>a</sup>

<sup>a</sup> Beijing National Laboratory of Molecular Sciences, Key Laboratory of Analytical Chemistry for Living Biosystems, Institute of Chemistry, Chinese Academy of Sciences, Beijing 100190, China

<sup>b</sup> Graduate School, Chinese Academy of Sciences, Beijing 100049, China

<sup>c</sup> College of Pharmacy, Hebei University, Baoding 071002, China

## ARTICLE INFO

### Article history:

Received 9 February 2010

Received in revised form

21 May 2010

Accepted 22 May 2010

Available online 1 June 2010

### Keywords:

Polymer monoliths

Amphiphilic diblock copolymer

Protein

## ABSTRACT

A novel type of amphiphilic diblock copolymer consisting of butyl methacrylate (BMA) block and glycidyl methacrylate (GMA) block (BG copolymer) was successfully synthesized *via* atom transfer radical polymerization (ATRP) and then utilized as a phase separator to control the porous structure of poly (butyl methacrylate-co-ethylene dimethacrylate) (poly(BMA-co-EDMA)) monoliths. It has been found that the addition of the BG copolymer had a great impact on the polymerization of the monoliths. When the amount of the BG copolymer added into the synthesizing solution was changed, the porous structure could be varied from aggregated microglobular structure to well-defined three-dimensional (3D) skeletal structure. The porous structure was characterized by scanning electron microscope, mercury intrusion porosimetry and nitrogen adsorption measurement. Finally, the separation of proteins demonstrated its potential applications in proteome research.

© 2010 Elsevier Ltd. All rights reserved.

## 1. Introduction

Rigid macroporous polymer monoliths emerged in the early 1990s and found their solid place in a large variety of fields, such as separation, catalysis, sensors, and solid-phase extraction [1,2], which depends on their uniform macroporous structure composed of interconnected repeating macropores or cells. Thereby, how to create a well-defined and homogeneous structure has been always the key point in the preparation of monolithic materials. In general, high separation efficiency can be more easily realized on monolithic columns with well-controlled skeletal structures. However, it is difficult to control the porous morphology of polymer monoliths prepared by traditional free radical polymerization because of the fast phase separation between the growing polymer chains and the porogenic solvents [2,3]. As a result, the porous structure of polymer monoliths obtained by this method was entirely featured with aggregated microglobules at micrometre scale. Furthermore, many adverse effects took place in the flow-through systems, *e.g.*, low permeability, larger eddy diffusion through irregular interstitial channels, limited pore surface area and heterogeneity of the molecular recognition site [4]. Therefore, it is a matter of great

concern to control the phase separation process in polymerization and create a more homogeneous porous structure.

To deal with the problem mentioned above, many research groups have made great efforts. Svec and co-workers have systematically investigated pore formation during the  $\gamma$ -radiation-initiated synthesis of porous polymer monoliths [5]. Eeltink and colleagues tailored the morphology of methacrylate ester-based monoliths to obtain optimum efficiency in liquid chromatography [6]. Because living radical polymerization could be used to optimize the porous structure, Svec and co-workers attempted polymerizing in the presence of 2,2,6,6-tetramethylpiperidin-1-yl oxide (TEMPO) [7]. Buchmeiser and colleagues prepared a new class of monoliths by ring-opening metathesis [8]. Then, Kanamori and co-workers presented a new term “phase separator” and prepared well-defined macroporous polymer networks *via* various types of living radical polymerization [9–12]. Although it was difficult and tedious to carry out living radical polymerization, Tanaka and colleagues displayed the basic study of the gelation of dimethacrylate-type crosslinking agents [13] and the poly(glycerin 1,3-dimethacrylate)-based monoliths with a fine bicontinuous network structure obtained by common free radical polymerization *via* viscoelastic phase separation [14,15]. They also studied the well-controlled 3D skeletal epoxy-based monoliths by polymerization induced phase separation [16]. However, a few reports concerned to use the molecules with ultra high molecular weight, such as polystyrene, as

\* Corresponding author. Tel: +86 10 82627290; fax: +86 10 62559373.  
E-mail address: [qjli@iccas.ac.cn](mailto:qjli@iccas.ac.cn) (L. Qi).

porogen [15] because these kinds of ultra high molecular weight “phase separators” were costly and not easy to find. In addition, the types of epoxy monomers were rather limited and it was difficult to carry out surface modification reactions on the epoxy-based monoliths, so that the application was restricted within narrow limits.

Herein, we explored to use amphiphilic diblock copolymers as a novel type of phase separator for controlling the phase separation in the polymerization. Amphiphilic diblock copolymers consisted of two chemically different polymer segments connected by a covalent linkage. When amphiphilic diblock copolymers were solved in selective solvents, they could form stable aggregates with a wide range of morphologies, including spheres, rods, lamellae, tubules, vesicles, microdomain alignment *etc* [17–21]. Therefore, a novel type of amphiphilic diblock copolymers, in which one block was composed of a polymer segment of the monomer used in the following preparation of monolithic polymers, was designed and successfully synthesized. Then the synthesized amphiphilic pBMA-b-pGMA (BG) copolymers were added into the polymerization mixture in order to modulate the interactions between the growing polymer chains and the porogenic solvents. Going along with the polymerization, the phase separation took place and a well-defined co-continuous structure could be induced by the diblock copolymer. When the polymerization was completed, this structure was chemically frozen. After the porogenic solvents were removed, the 3D skeletons and macropores were left (Scheme 1). Through mercury intrusion measurement and N<sub>2</sub> adsorption, hierarchically porous structure was demonstrated, which benefits a lot to the chromatographic applications. Finally, the poly(butyl methacrylate-*co*-ethylene dimethacrylate) (poly(BMA-*co*-EDMA)) monolithic column was successfully utilized to separate proteins.

## 2. Experimental section

### 2.1. Chemicals

Glycidyl methacrylate (GMA), ethylene glycol dimethacrylate (EDMA) and n-butyl methacrylate (BMA) were purchased from Acros company (New Jersey, USA) and purified before use. Azobisisobutyronitrile (AIBN) was produced by Shanghai Chemical Plant (Shanghai, China) and refined by recrystallization from the methanol before use. Tetrahydrofuran (THF), acetonitrile (ACN),

2,2'-bipyridyl, methanol, cyclohexanone, dodecanol, ethyl 2-bromopropionate, trifluoroacetate (TFA) and CuBr were purchased from Beijing Chemical Plant (Beijing, China) and used without further purification. Cytochrome C (Cyt-C), ribonuclease A (RNase-A) and myoglobin (Myo) were obtained from Sigma–Aldrich company (Louis, USA).

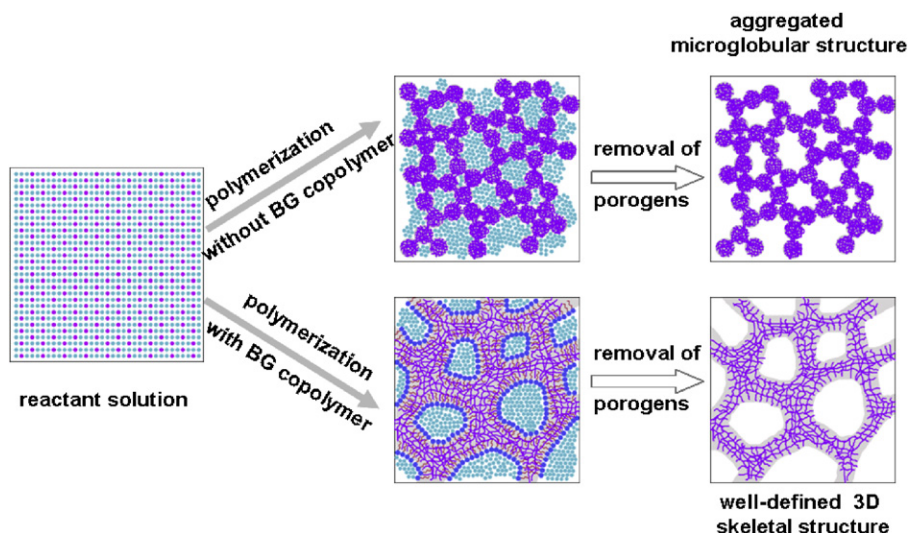
### 2.2. Preparation and characterization of amphiphilic diblock copolymers

The amphiphilic diblock copolymers were prepared by atom transfer radical polymerization (ATRP). The polymerizations were conducted in pre-dried round-bottom flasks. CuBr and 2,2'-bipyridyl were added and the flask was tightly closed with a rubber septum. After the air was removed by evacuation and purging with ultra pure N<sub>2</sub> (three cycles), a mixture of BMA, cyclohexanone, and ethyl 2-bromopropionate was added *via* syringe after being purged with ultra pure N<sub>2</sub> for 15 min. The mixture was stirred for 10 min and then placed in a pre-heated oil bath at 55 °C. After the polymerization was carried out for 24 h under the protection of nitrogen, the second monomer GMA was added and the polymerization continued for another 24 h as described above. Then the flask was removed from the oil bath and the amphiphilic diblock copolymer was isolated by precipitation into methanol. The precipitation was repeated for three times.

### 2.3. Preparation of rigid macroporous monoliths

The prepared amphiphilic BG copolymer was dissolved in cyclohexanone and then the amphiphilic BG copolymer solution was added into the mixture of BMA, EDMA, and dodecanol. The polymerization mixture was thermally initiated by AIBN at 60 °C in a dried glass bottle. After 24 h polymerization, the bulk samples were transferred to Soxhlet extractor to remove the templated polymers and other soluble compounds using THF for 72 h, followed by vacuum-drying at 50 °C overnight.

As a control experiment, a macroporous monolith was also prepared without amphiphilic BG copolymers. Another control experiment was also carried out by adding a mixture of pBMA and pGMA (two homopolymers), the molecular weight of which are the same as each block of a block copolymer, instead of amphiphilic BG copolymers.



**Scheme 1.** The mechanism of the well-defined skeletal macroporous polymer monoliths.

For chromatography use, the monolithic polymer was prepared in a 4.6 mm i.d.  $\times$  100 mm stainless steel column. After polymerization for 24 h, the monolithic column was connected to the HPLC pump to wash out the porogen and unreacted monomers with THF before the chromatographic use.

#### 2.4. Characterization of the porous property of the well-defined skeletal monolithic polymers

For scanning electron microscope (SEM) observation, the dried polymer samples were snapped apart and placed on sticky copper foil, which was attached to a standard aluminum specimen stub. The polymer was coated with about 10 nm of gold by Eiko IB-3 sputter coating (Eiko, Engineering Co. Ltd., Japan). Microscopic analysis was carried out with a HITACHI S-4800 SEM (Hitachi High Technologies, Japan).

The porous property of the well-defined skeletal monolithic polymers was characterized by mercury porosimetry and nitrogen sorption. Mercury porosimetry (AUTOPORE II 9220, Micromeritics, USA) was used to characterize the macroporous character of the rigid macroporous monoliths, whereas nitrogen adsorption–desorption (ASAP-2020, Micromeritics, USA) was employed to characterize the meso- and micro-porous character of these monolithic polymers.

For mercury porosimetry, the pore sizes were characterized using the Washburn equation assuming a cylindrical shape for the pores. For nitrogen adsorption, the adsorption–desorption isotherm was calculated by BET method and the pore size distribution was calculated by Barrett–Joyner–Halenda (BJH) method using the adsorption branch of each isotherm. The samples were degassed at 200 °C under vacuum for at least 1 h prior to the nitrogen sorption measurements.

#### 2.5. Separation of proteins

Separation of proteins was applied on the resulting monolithic column with a Shimadzu Prominence 20A HPLC system consisting of a binary LC-20AT HPLC pump and an SPD-20A UV–Vis Detector. Mobile phase gradient was set as: Eluant A: 90% H<sub>2</sub>O/10% ACN v/v, 0.1% TFA; Eluant B: 10% H<sub>2</sub>O/90% ACN v/v, 0.1% TFA; gradient: 0% B (0 min) to 30% B in 3 min, 30% B to 65% B in 7 min. The flow rate was 0.5 mL/min. The proteins were detected at a UV wavelength 280 nm. Data processing was performed with HW-2000 chromatography workstation (Nanjing Qianpu Software, China).

### 3. Results and discussion

#### 3.1. Preparation and characterization of amphiphilic BG copolymers

At the beginning of this work, amphiphilic BG copolymers were synthesized *via* ATRP, which are controlled/living polymerization affording polymers with differing compositions (i.e., random, periodic, graft, block, gradient, etc.) and narrow molecular weight distribution. To investigate the influence of the block ratio on the porous morphology of the resulting monolithic polymer, amphiphilic BG copolymers with three block ratios were prepared. They were p(BMA)<sub>70</sub>-b-(GMA)<sub>10</sub> (BG-1), p(BMA)<sub>70</sub>-b-(GMA)<sub>70</sub> (BG-2), p(BMA)<sub>20</sub>-b-(GMA)<sub>70</sub> (BG-3), respectively.

To confirm the composition of amphiphilic BG copolymers was the same as designed, the structure of the amphiphilic BG copolymers was characterized by nuclear magnetic resonance (NMR) and gel permeation chromatography (GPC). The results of BG-1 were displayed in Figs. 1 and 2. The GPC result of BG-1 shows that  $M_n$  was at  $1.22 \times 10^4$  and the polydispersity index (PDI) was 1.28. According to the <sup>1</sup>H NMR result shown in Fig. 2

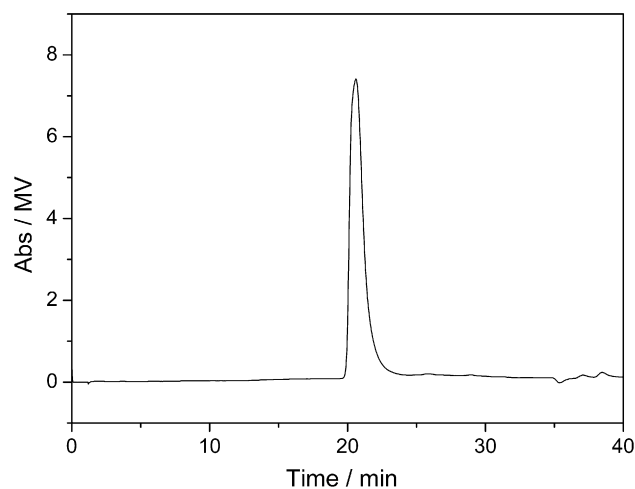


Fig. 1. GPC results of BG-1.

(numbers in the structure formula correspond to assignments in the NMR spectrum), the block ratio of BG-1 was 71/9, which was very close to the theoretical value (70/10). To further confirm that it was a perfect amphiphilic diblock copolymer, we had benefited from another GPC result. Before the second monomer was added, the homopolymer of the first monomer was taken out, purified and then checked by GPC. The GPC result indicated that the first monomer was almost completely consumed. Therefore, the homopolymerization of the first monomer was carried out at 55 °C for 24 h to get a diblock copolymer as expected.

These results indicated that amphiphilic BG copolymer was successfully synthesized and the block ratio could be controlled *via* ATRP method, which provided a solid foundation for the following preparation of well-defined macroporous monoliths. Therefore, based on the controllable property of ATRP in the composition, topology, or the functional groups of the polymer, various kinds of block copolymers could be prepared as designed to fit different monomers used in the preparation of polymer monoliths. In another word, this method could be extended to other commonly used monomers to create polymer monoliths with 3D skeletal macroporous structure as long as suitable amphiphilic BG copolymers could be designed and synthesized.

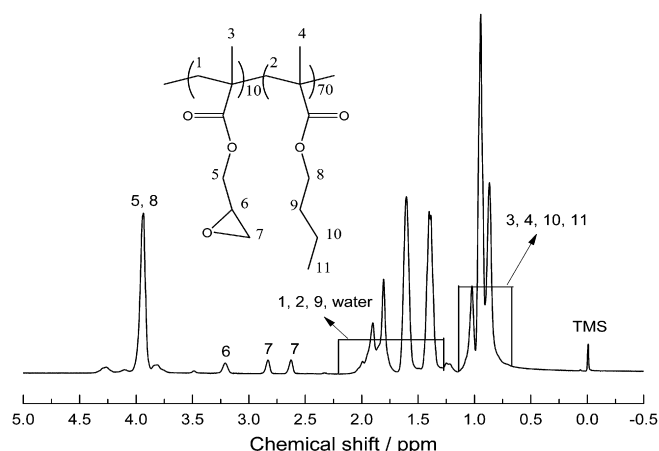


Fig. 2. <sup>1</sup>H NMR results of BG-1 in CDCl<sub>3</sub>.



### 3.2. Preparation of rigid macroporous poly(BMA-co-EDMA) monoliths

Macroporous poly(BMA-co-EDMA) monoliths were prepared *in situ* with the prepared amphiphilic BG copolymers (Table 1s). After polymerization, microstructures of the dried monoliths have been observed by SEM (Fig. 1s). Fig. 3 reveals the morphology changes due to the varied doses of amphiphilic BG copolymers and different amphiphilic BG copolymer solution/dodecanol ratios (v/v). First of

all, the role of amphiphilic BG copolymers in the polymerization was validated. Fig. 3a is the SEM image of the monolithic polymer prepared without amphiphilic BG copolymers, which is obviously featured with interconnected micoglobules. With the addition of BG-1, the morphology changed. When the BG-1 solution/dodecanol ratio was low, the aggregated microglobular structure seemed to be similar to Fig. 3a. However, there still remained some differences that the microglobule became much smaller and coarser, and those microglobules tended to transform into a 3D skeletal structure

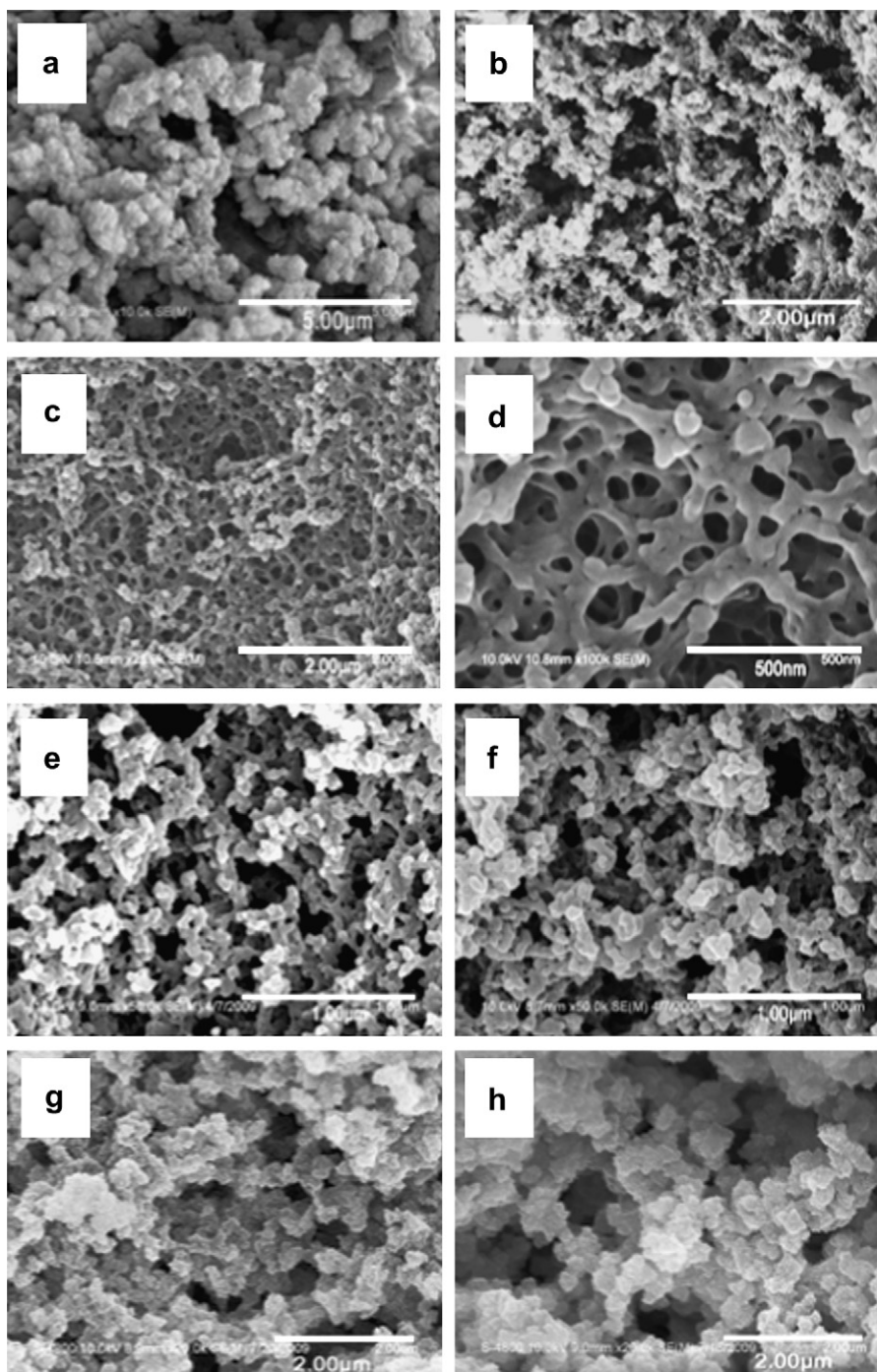


**Fig. 3.** SEM images of poly(BMA-co-EDMA) macroporous monoliths. a) Porogen% = 75 vol.%, cyclohexanone/dodecanol = 1/9 (v/v); b) Porogen% = 75 vol.%, BG-1 (5% w/v)/dodecanol = 1/9 (v/v); c,d) Porogen% = 75 vol.%, BG-1 (5% w/v)/dodecanol = 1/4 (v/v); e) Porogen% = 67 vol.%, BG-3 (10% w/v)/dodecanol = 1/9 (v/v); f) Porogen% = 67 vol.%, BG-2 (10% w/v)/dodecanol = 1/4 (v/v); g) Porogen% = 75 vol.%, (p(GMA)<sub>10</sub> + p(BMA)<sub>70</sub>) (5% w/v)/dodecanol = 1/4 (v/v); h) Porogen% = 67 vol.%, (p(GMA)<sub>70</sub> + p(BMA)<sub>70</sub>) (10% w/v)/dodecanol = 1/9 (v/v).

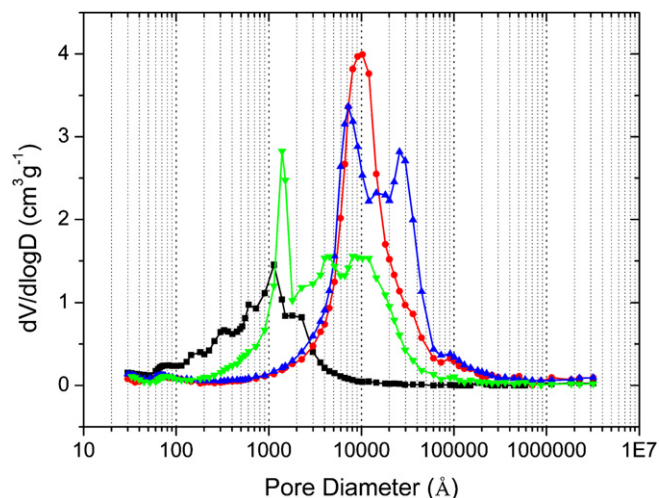


**Fig. 4.** Macropore size distributions of rigid macroporous monoliths obtained with different porogen compositions, measured by mercury intrusion porosimetry. ▲ Porogen% = 67 vol.%, BG-1 (10% w/v)/dodecanol = 1/16 (v/v); porosity = 62.93%; ● Porogen% = 75 vol.%, BG-1 (5% w/v)/dodecanol = 1/9 (v/v); porosity = 74.56%; ■ Porogen% = 75 vol.%, BG-1 (20% w/v)/dodecanol = 1/2 (v/v); porosity = 78.70%; ▼ Porogen% = 75 vol.%, BG-2 (10% w/v)/dodecanol = 1/9(v/v); porosity = 75.27%.

(Fig. 3b). When the BG-1 solution/dodecanol ratio was increased, the morphology changed drastically to a bicontinuous skeletal structure (Fig. 3c and d) and the skeletons were sized in about 100 nm. However, when BG-2 solution /dodecanol ratio equaled 1/4 (Fig. 3f) or BG-3 solution /dodecanol ratio equaled 1/9 (Fig. 3e) the porous structure was rather close to aggregated microglobular structure than 3D skeletal structure. In another word, the block ratio of the amphiphilic BG copolymers indeed played the key role on the transformation point.

To further confirm the role of the amphiphilic BG copolymers and eliminate the concern, another control experiment was carried out. Fig. 3g and h depict the SEM images of the monoliths prepared with a mixture of pBMA and pGMA (two homopolymers), the molecular weight of which are the same as each block of a block copolymer, instead of BG copolymers. The results demonstrated that the amphiphilic BG copolymers played a key role in the morphology change. The reason for this phenomenon may be that the homopolymers couldn't act on the interface between the porogen phase and the polymer phase in the phase separation process. In addition, under some conditions when pGMA concentration was increased and the molecular weight of pGMA was high,

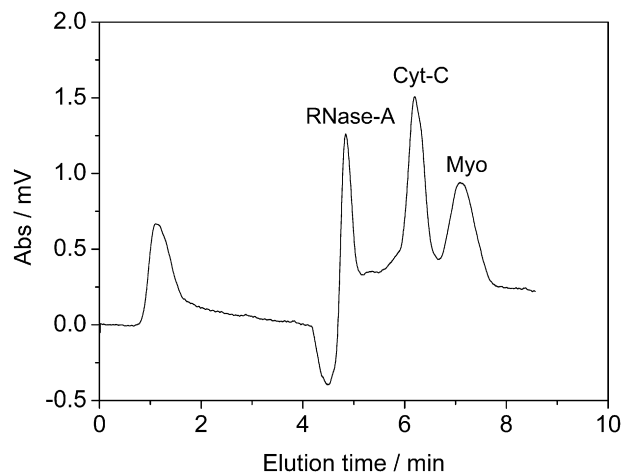


**Fig. 6.** Separation of proteins on the P(BMA-co-EDMA) monoliths in RP-HPLC mode. Peaks: 1. RNase-A; 2. Cyt-C; 3. Myo.

pGMA precipitated and then the mixture became a non-homogeneous solution.

The formation of the well-defined skeletal morphology and the transformation can be explained by the mean-field theory [22]. According to this theory, the free energy change of mixing is described as:

$$\Delta G \propto RT \left( \frac{\phi_1}{P_1} \ln \phi_1 + \frac{\phi_2}{P_2} \ln \phi_2 + \chi \phi_1 \phi_2 \right) \quad (1)$$

Where  $\phi_i$  and  $P_i$  are the volume fraction and DP (degree of polymerization) of component  $i$  ( $i = 1$  or  $2$ ) and  $\chi$  is the interaction parameter, which represents the interaction between component 1 and 2. The parameter  $\chi$  is also proportional to the difference between the solubility parameters of the two components. Assuming component 1 and 2 are the BMA-co-EDMA derived species and the porogenic solvents respectively, the first entropy term  $\phi_1/P_1 \ln \phi_1$  becomes less negative with the polymerization going on, but for both polymerization systems with and without addition of the amphiphilic BG copolymers, the  $\phi_1/P_1 \ln \phi_1$  value almost equals each other because the amphiphilic BG copolymer dosage was little. In contrary, the second entropy term  $\phi_2/P_2 \ln \phi_2$  remains constant for both systems because  $\phi_2$  and  $P_2$  of the porogenic solvents are constant. Nevertheless, the addition of the amphiphilic BG copolymers, in which one block was constituted of the polymer segment of the monomer, strengthened the

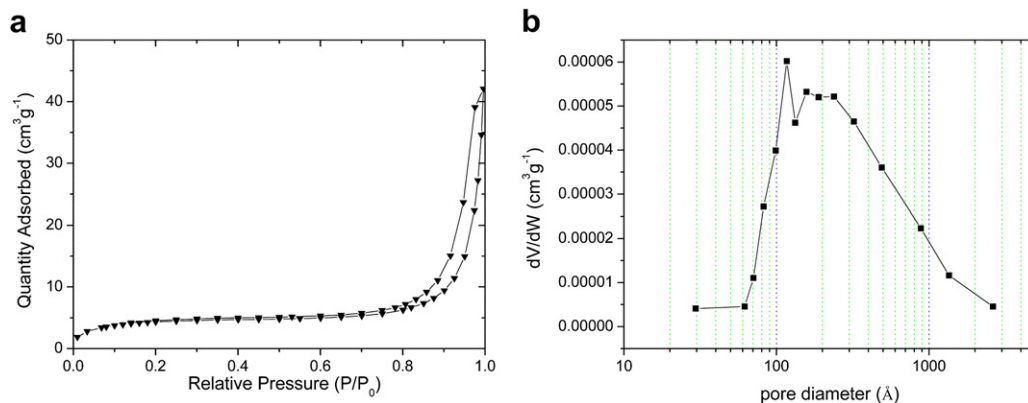


**Fig. 5.** a. BET adsorption-desorption isotherm; b. mesopore size distribution.

interaction between the growing polymer chains and the porogenic solvent molecules and lowered the last enthalpy term  $\chi\phi_1\phi_2$  drastically. As a result, the free energy change of mixing decreased and the phase separation process was delayed, which easily led to a well-defined skeletal structure.

The porous property of the rigid macroporous monoliths was further studied by mercury intrusion porosimetry and nitrogen adsorption. Mercury intrusion porosimetry gave the porosity values at 62.93%, 74.56%, 78.70% and 75.27%, which were very close to the volume fraction of the porogenic solvents in the feed polymerization solution. The result indicates that the resultant monolithic polymers have almost no shrinkage even in dry state and are suitable for chromatographic applications. In addition, the highly porous structure made the material tolerate fast flow rates although the average pore size was a little smaller than those traditional polymer monoliths. The macropore size distribution profiles of four samples have been depicted in Fig. 4. It can be observed that the mode pore diameter of these monolithic polymers varied from 100 nm to 1  $\mu\text{m}$  (Fig. 4), which implies that the amphiphilic BG copolymers didn't only influence the porous morphology of the resultant monolithic polymer, but also played a role on the macropore size distribution.

Additionally, the nitrogen adsorption–desorption isotherm (Fig. 5a) was featured with adsorption hysteresis, indicative of the presence of mesopores, which could be validated by the mesopore size distribution measured by BJH method (Fig. 5b). Furthermore, the adsorption hysteresis exhibited Type H3 loop, which was associated with narrow slit-like pores.

### 3.3. Application of the monolith to RP-HPLC

Due to the fast mass transfer and high column efficiency, monolithic macroporous polymers have advantages in the separation of large biomolecules. As shown in Fig. 6, a protein mixture constituted of Cyt-C, RNase-A and Myo was well separated on the poly(BMA-co-EDMA) based monolithic column. It should be pointed out that the mixture was separated in reversed phase liquid chromatography mode (RP-HPLC) because of the strong hydrophobicity of the pore surface. The unmarked peaks present the solvent and impurities in the protein sample. This successful case also demonstrated its potential applications in proteome research.

## 4. Conclusion

The amphiphilic BG copolymer is an effective phase separator to control the phase separation and further influence the porous morphology of the resulting monolithic polymers. In addition, this method could be extended to a lot of monomers to create 3D skeletal structure because different amphiphilic diblock

copolymers could be designed and synthesized to fit different monomers. With the adjustment of the BG copolymer dosage and the BG copolymer solution/poor solvent ratio, polymer monoliths with sub-micron skeletons and uniform macropores could be obtained. Meanwhile, mesopores at several nanometers scale could also be created on the skeletons. Therefore, this hierarchically porous structure can afford the monolithic polymer with fast mass transfer and also large adsorption capacity, which is important when this monolithic material used in flow-through systems.

## Acknowledgements

The authors are grateful for the financial support from Ministry of Science and Technology of China (No. 2007CB714504), NSFC (No. 20875091 and No. 20935005) and Chinese Academy of Sciences.

## Appendix. Supporting information

Supporting information associated with this article can be found, in the online version, at [doi:10.1016/j.polymer.2010.05.043](https://doi.org/10.1016/j.polymer.2010.05.043).

## References

- [1] Svec F, Tennikova TB, Deyl Z. Monolithic materials: preparation, properties and application. In: J Chromatogr Libr, vol. 67. Amsterdam: Elsevier; 2003.
- [2] Zhang RY, Qi L, Xin PR, Yang GL, Chen Y. Polymer 2010;51(8):1703–8.
- [3] Tsujioka N, Hira N, Aoki S, Tanaka N, Hosoya K. Macromolecules 2005;38(24):9901–3.
- [4] Guiochon G. J Chromatogr A 2007;1168(1–2):101–68.
- [5] Sáfrány Á, Beiler B, László K, Svec F. Polymer 2005;46(9):2862–71.
- [6] Eeltink S, Schoenmakers PJ, Kok WT. Anal Chem 2005;77(22):7342–7.
- [7] Viklund C, Irgum K, Svec F, Frechet JMJ. Macromolecules 2001;34(13):4361–9.
- [8] Sinner F, Buchmeiser MR. Macromolecules 2000;33(13):5777–86.
- [9] Kanamori K, Nakanishi K, Hanada T. Adv Mater 2006;18(18):2407–11.
- [10] Hasegawa J, Kanamori K, Nakanishi K, Hanada T, Yamago S. Macromolecules 2009;42(4):1270–7.
- [11] Hasegawa J, Kanamori K, Nakanishi K, Hanada T, Yamago S. Macromol Rapid Commun 2009;30(12):986–90.
- [12] Kanamori K, Hasegawa J, Nakanishi K, Hanada T. Macromolecules 2008;41(19):7186–93.
- [13] Aoki H, Hosoya K, Tanaka N, Nakanishi K. J Polym Sci Part A Polym Chem 2006;44(2):949–58.
- [14] Aoki H, Kubo T, Ikegami T, Tanaka N, Hosoya KN, Tokuda D, et al. J Chromatogr A 2006;1119(1–2):66–79.
- [15] Aoki H, Tanaka N, Kubo T, Hosoya K. J Polym Sci Part A Polym Chem 2008;46(14):4651–73.
- [16] Tsujioka N, Ishizuka N, Tanaka N, Kubo T, Hosoya K. J Polym Sci Part A Polym Chem 2008;46(10):3272–81.
- [17] Yu K, Eisenburg A. Macromolecules 1998;31(11):3509–18.
- [18] Jain S, Bates FS. Science 2003;300(5618):460–4.
- [19] Böker A, Elbs E, Hänsel H, Knoll A, Ludwigs S, Zettl H, et al. Phys Rev Lett 2002;89(13):135502-1–4.
- [20] Wang DR, Liu JP, Ye G, Wang XG. Polymer 2009;50(2):418–27.
- [21] Wang L, Hu P, Tirelli N. Polymer 2009;50(13):2863–73.
- [22] Flory PJ. Principles of polymer chemistry. Ithaca, NY: Cornell University Press; 1971.